J. Fluid Mech. (1971), *vol.* **45**, *part* 1, *pp.* 161–187
Printed in Great Britain

The three-dimensional distributions of tangential velocity and total-temperature in vortex tubes

By C. U. LINDERSTRØM-LANG
Research Establishment Risö, Roskilde, Denmark

(Received 16 December 1969 and in revised form 12 June 1970)

The axial and radial gradients of the tangential velocity distribution are calculated from prescribed secondary flow functions on the basis of a zero-order approximation to the momentum equations developed by Lewellen. It is shown that secondary flow functions may be devised which meet pertinent physical requirements and which at the same time lead to realistic tangential velocity gradients.

The total-temperature distribution in both the axial and radial directions is calculated from such secondary flow functions and corresponding tangential velocity results on the basis of an approximate turbulent energy equation. The method employed for the solution of this equation stresses the equivalence of the vortex tube to counter-current systems with transverse diffusion such as distillation columns and heat exchangers.

An availability function is derived that permits the evaluation of vortex tube performance on the basis of velocity data.

Turbulent diffusivities resulting from the quantitative use of the tangential velocity approximation are shown to agree with those derived from the total-temperature calculations.

1. Introduction

The theory of the tangential velocity distribution in the vortex tube has been treated previously but primarily in relation to tubes with a large radial influx of fluid. For this case a satisfactory link between circulation and radial Reynolds number has been established on the assumption that the flow conditions in the tube, excluding boundary layers, are independent of axial position (Rosenzweig, Ross & Lewellen 1962).

In longer vortex tubes with inlet nozzles at only one end, the above (quasi-) two-dimensional approach is no longer useful since, on the one hand, the tangential velocity takes a shape close to that of the forced vortex, and on the other hand, it shows a significant axial gradient; at the same time the radial velocity drops considerably and becomes much lower than the axial velocity.

A solution to this problem has been derived by Lewellen (1964) for the incompressible case as an extension of a study of tubes in which the radial and axial

flows were of the same order of magnitude (Lewellen 1962). In the present work the zero-order approximation of this expansion is examined. For that purpose the equations have been transformed and expressed in terms of experimentally available parameters.

It should be noted that the theory is developed for incompressible fluid flow while the examples used are compressible fluid cases. As shown by Anderson (1963) and Rosenzweig, Lewellen & Ross (1964) this may not lead to serious errors under conditions of interest here.

A complete theoretical description of the temperature distribution in the vortex tube is a very complex problem, owing to its three-dimensional character. However, Reynolds (1961) and Bruun (1967, 1969) discussing the relative importance of the turbulent contributions to the separation effect, have reached a qualitative understanding of the mechanism. Furthermore, attempts have been made to calculate the radial temperature gradient using essentially two-dimensional methods (Deissler & Perlmutter 1960; Hartnett & Eckert 1957; Takahama 1965), while in other cases the influence of the axial temperature gradient has been studied (Fulton 1950; Gulyaev 1966; Kassner & Knoernschild 1948; Lay 1959; Scheper 1951; Sibulkin 1962; Suzuki 1960).

The present approach permits both axial and radial gradients of the temperature to be taken into account in a comparatively simple and accurate way. The discussion is limited to long tubes with weak radial inflow as is the section on the velocity distribution. The treatment is based on a simplified energy equation which has been derived earlier by Reynolds (1961) and Bruun (1967, 1969). For the solution of this equation, which is a partial differential equation in the axial and radial co-ordinates, a method closely related to the one employed for mass separation in two-component gas mixtures in rotating flow (Cohen 1951) is used. As a step in the solution, a first-order differential equation in the axial co-ordinate is obtained, which is equivalent to the governing equation for an ordinary counter-current heat exchanger. Previous workers have already noted the equivalence of the counter flow in vortex tubes to counter-current heat-exchangers (Scheper 1951; Suzuki 1960; Gulyaev 1966) and used it for a description of the separation process; assumptions about the heat exchange rate across the boundary between the streams have been made and mean values of stream temperature employed. In the present approach no assumptions about the rate of heat exchange, except that it is proportional to the turbulent thermal diffusivity, are necessary. Furthermore, sufficient information is embodied in the first-order differential equation that an approximation to both the radial and axial temperature gradients is obtained as a result of the calculations.

In the study, the total temperature is employed as the dependent variable with the total-enthalpy as the quantity transported. The velocity field is assumed to be known throughout the tube region under consideration. This region does not include any boundary layers; it is identical with the region considered in the velocity study (§ 2). The analytical results obtained in that section concerning velocity distributions are applied in the temperature study.

It is generally accepted that the vortex tube is a wasteful cooling machine; it has not, however, been completely clear why this must be so. Here, an equation,

which exposes the performance criteria quite well, is derived on the basis of an approximate availability function and with the use of the energy equation adopted in the temperature study.

2. The tangential velocity distribution

2.1. *Theory*

The governing equations are the continuity equation and the Navier–Stokes equations for the velocity components in cylindrical co-ordinates. From these four equations Lewellen (1962) eliminates the pressure, introduces the circulation $2\pi\tilde{\Gamma} = 2\pi\tilde{v}r$ and the axisymmetric stream function

$$\partial\tilde{\psi}/\partial z \equiv ur \quad \text{and} \quad \partial\tilde{\psi}/\partial r \equiv -wr \tag{1}$$

and obtains the following two partial differential equations where all quantities are dimensionless

$$\frac{\partial\psi}{\partial\xi}\frac{\partial\Gamma}{\partial\eta} - \frac{\partial\psi}{\partial\eta}\frac{\partial\Gamma}{\partial\xi} = \frac{2\eta}{Re}\frac{\partial^2\Gamma}{\partial\eta^2} + \frac{\alpha}{2Re}\frac{\partial^2\Gamma}{\partial\xi^2}, \tag{2}$$

$$\Gamma\frac{\partial\Gamma}{\partial\xi} = Ro^2\left\{4\eta^2\left[\frac{\partial\psi}{\partial\xi}\frac{\partial^3\psi}{\partial\eta^3} - \frac{\partial\psi}{\partial\eta}\frac{\partial^3\psi}{\partial\xi\,\partial\eta^2} - \frac{2}{Re}\left(2\frac{\partial^3\psi}{\partial\eta^3} + \eta\frac{\partial^4\psi}{\partial\eta^4}\right)\right]\right.$$
$$\left. + \alpha\left[-\frac{\partial\psi}{\partial\xi}\frac{\partial^2\psi}{\partial\xi^2} + \eta\frac{\partial\psi}{\partial\xi}\frac{\partial^3\psi}{\partial\eta\,\partial\xi^2} - \eta\frac{\partial\psi}{\partial\eta}\frac{\partial^3\psi}{\partial\xi^3} - \frac{1}{Re}\left(4\eta^2\frac{\partial^4\psi}{\partial\eta^2\,\partial\xi^2} + \frac{\alpha}{2}\eta\frac{\partial^4\psi}{\partial\xi^4}\right)\right]\right\}. \tag{3}$$

Here $\Gamma \equiv \tilde{\Gamma}/\Gamma_s$ and $\psi \equiv \tilde{\psi}/\psi_s$ are normalized circulation and stream functions respectively; $\xi \equiv z/z_s$ is a normalized axial position and $\eta \equiv (r/r_s)^2$ measures the radial position as the square of a normalized radius. Furthermore,

$$Ro \equiv \psi_s/(\Gamma_s r_s) \quad \text{and} \quad Re \equiv \psi_s/(\nu_s z_s)$$

are Rossby and Reynolds numbers respectively, while $\alpha \equiv (r_s/z_s)^2$ is the square of a ratio of characteristic lengths. ν is the kinematic viscosity; it is generally accepted that the flow in the tubes is turbulent; it will be assumed below that the above equations apply to this case unaltered with Re interpreted as a constant turbulent Reynolds number.

With a suitable choice of reference parameters Lewellen (1964, p. 91) has discussed the series expansion of (2) and (3) in terms of the Rossby number, under conditions where $u \ll w \ll v$. In Linderstrøm-Lang (1970*a*) (referred to as (I) below) the resulting zero-order approximation has been transformed on the basis of the following set of reference parameters (cf. figure 1)

$$r_s \equiv r_p, \quad z_s \equiv l, \quad \Gamma_s \equiv \tilde{\Gamma}_{p0} \equiv \tilde{v}_{p0} r_p, \quad \text{and} \quad \psi_s \equiv F, \tag{4}$$

where r_p is the tube radius, l the length of the tube section under consideration, i.e. the length of region I (figure 1) which, as will become clear below, can be chosen arbitrarily. $2\pi\tilde{\Gamma}_{p0}$ is the circulation at the periphery near the nozzle (and $\tilde{v}_{p0}$ the corresponding tangential velocity). $2\pi F$ is the total volume flow through the tube. The resulting equations are

$$\frac{2\eta}{Re}\frac{1}{\sqrt{\alpha}}\Gamma_0'' + f_{00}'\Gamma_{11} - \frac{Re_r}{Re\sqrt{\alpha}}f_{11}\Gamma_0' = 0, \tag{5}$$

$$\Gamma_0\Gamma_{11} = 4\eta^2 Ro^2\left[f_{00}'''\frac{Re_r}{Re\sqrt{\alpha}}f_{11} - f_{00}'\frac{Re_r}{Re\sqrt{\alpha}}f_{11}'' - \frac{2}{Re}\frac{1}{\sqrt{\alpha}}(2f_{00}''' + \eta f_{00}^{\mathrm{iv}})\right]. \tag{6}$$

Here $$Ro \equiv F/(\Gamma_{p0} r_p), \quad Re\sqrt{\alpha} \equiv F/(\nu l) = F/(\nu r_p) \times \sqrt{\alpha}, \tag{7}$$

while $\alpha \equiv (r_p/l)^2$, $\eta \equiv (r/r_p)^2$, and $\xi \equiv z/l$; furthermore, in (2) and (3) Γ and ψ are approximated by

$$\left.\begin{aligned} \Gamma &= \Gamma_0 + \Gamma_{11}\xi, \\ \psi &= f_{00} + \frac{Re_r}{Re\sqrt{\alpha}} f_{11}\xi, \end{aligned}\right\} \tag{8}$$

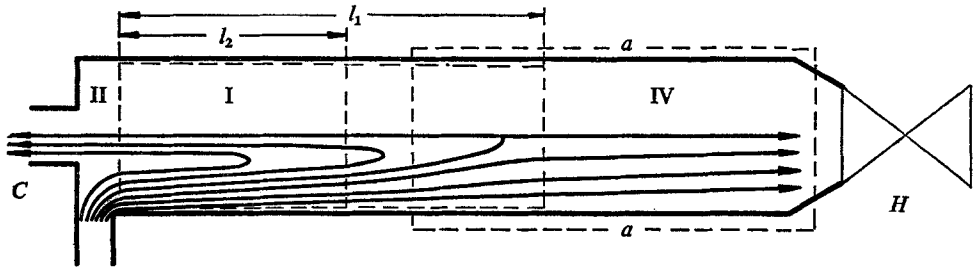

(a)

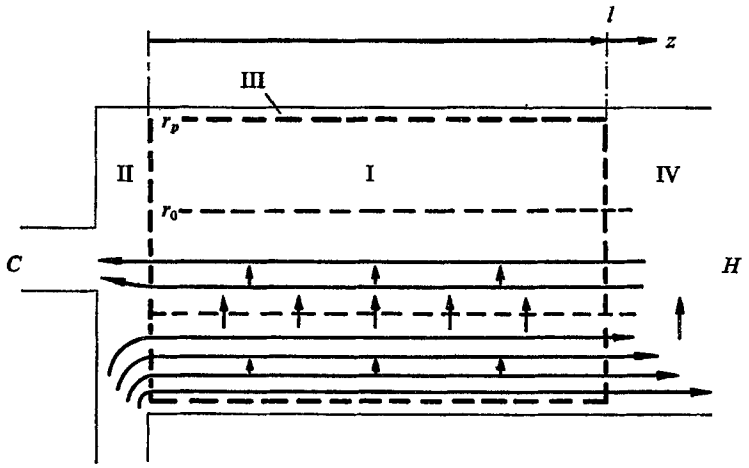

(b)

FIGURE 1. (a) Vortex tube with schematic stream line pattern and boundary of region I (two possibilities indicated). (b) Diagram of region I; arrows indicate axial and radial flow components.

where Γ_0, Γ_{11}, f_{00}, and f_{11} are functions of η. Re_r is a radial Reynolds number so chosen that $Re_r/(Re\sqrt{\alpha})$ is the ratio of the total radial volume flow at r_0, the radius at which the axial velocity changes sign, to the total volume flow through the tube ($2\pi F$).

The validity of (5) and (6) is restricted to $\Gamma_{11} \ll 1$ and $Re_r/Re\sqrt{\alpha} \times f_{11} \ll 1$ (see Lewellen 1964). This may be achieved in the experimental cases to be considered by restricting attention to short tube lengths, i.e. by choosing $\sqrt{\alpha}$ large enough; that Γ_{11} is reduced by this choice is seen by inspection of (5) and (6) where $\sqrt{\alpha}\,\Gamma_{11}$ is invariant to changes in $\sqrt{\alpha}$.

$2\pi\Gamma_{11}$ is seen from (8) to be the axial gradient of the circulation. Setting $\Gamma_{11} = 0$ in (5) gives the zero-order approximation employed in previous two-dimensional treatments (e.g. Deissler & Perlmutter 1960). Γ_0 describes the shape of the circulation in the radial direction, at $\xi = 0$. $f_{11}(\propto ur)$ determines the shape of the radial flow function in the radial direction ($f_{11} = 1$ at $\eta = \eta_0$, i.e. $r = r_0$), while f'_{00} ($\equiv \partial f_{00}/\partial\eta \propto w$) describes the axial flow as a function of η, at $\xi = 0$.

2.2. *Results*

In order to solve the equations presented above with respect to Γ suitable secondary flow functions, f_{00} and f_{11}, have been devised; details are given in (I). Here it suffices to stress that the successful use of equations (5) and (6) is condi-

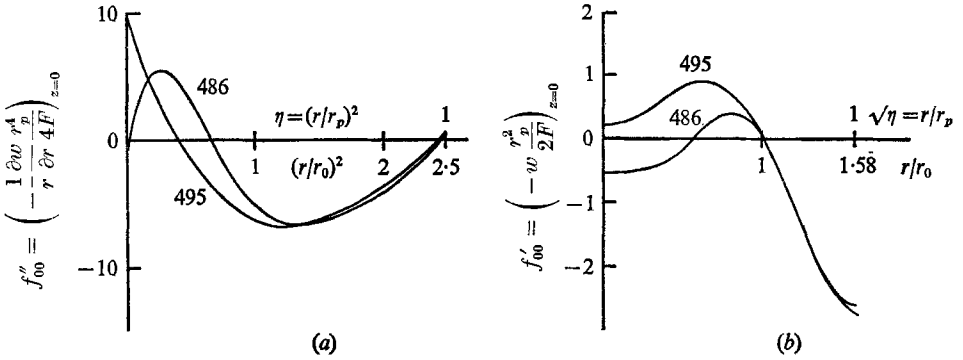

FIGURE 2. (*a*) Typical examples of prescribed f''_{00} functions plotted against η. (*b*) The same integrated with respect to η to yield the axial velocity function f'_{00}; abscissa $\sqrt{\eta}$. $1/\eta_0 = (r_p/r_0)^2 = 2{\cdot}5$. Case 486, cold flow fraction $\mu = 0{\cdot}034$; case 495, $\mu = 0{\cdot}252$.

tional on the existence of f_{00} functions that meet the rather restrictive requirements imposed upon them. First, that the resulting Γ_{11} must show certain characteristic features common to almost all experimental Γ distributions, namely, that Γ decreases along the tube within an annulus bounded approximately by $\eta = \eta_0$ (where w changes sign) and the periphery (figure 1), while it has a tendency to increase in the inner cylinder. These conditions limit the shape of $f''_{00}(\propto (1/r)\,\partial w/\partial r)$ to patterns such as those shown in figure 2(*a*). In addition, it is necessary that $f'_{00} = 0$ at η_0 (where $w = 0$), and, from a mass-balance consideration, that

$$\int_0^1 f'_{00}\,d\eta = -(1-\mu)$$

(where μ is the cold flow fraction, i.e. the fraction of flow through the cold exit (figure 1)). Furthermore, in accordance with experiment, the axial velocity, w, shall have a maximum (and therefore f'_{00} a minimum) at, or close to, the periphery. Finally, the boundary of region I is so chosen, that the total volume flow through the region enters at $\xi = 0$ between the radius where the axial velocity is zero and the periphery, i.e. that

$$\int_{\eta_0}^1 f'_{00}\,d\eta = -1.$$

Examples of axial flow functions, f'_{00}, for two different cold flow fractions are given in figure 2(*b*).

The radial flow function, f_{11} (equation (8)), which is not well determined experimentally, has been approximated by an exponential function in η with a maximum at η_0 and falling off to zero at the axis, and to a negligible level at

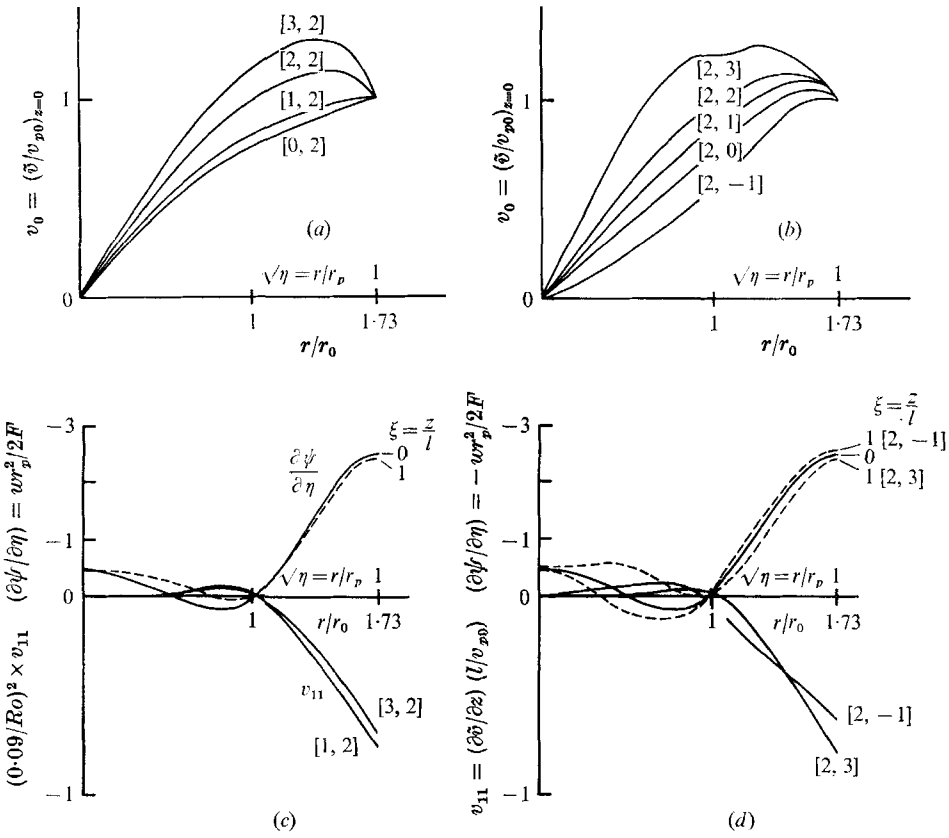

FIGURE 3. (*a*), (*b*) Non-dimensional tangential velocity $v_0 = \Gamma_0/\sqrt{\eta}$; and (*c*), (*d*), non-dimensional tangential velocity gradient $v_{11} = \Gamma_{11}/\sqrt{\eta}$; as functions of $\sqrt{\eta}$. Also shown, corresponding secondary flow functions, $\partial\psi/\partial\eta$, at $\xi = 0$ and $\xi = 1$. $Re\sqrt{\alpha}$ (equation (7)) = 15, $\mu = 0{\cdot}01$, $1/\eta_0 = 3$.

(*a*) and (*c*). Ratio of radial flow to total flow (equation (8)) $Re_r/Re\sqrt{\alpha} = 0{\cdot}055$;

Ro (equation (7))	0	0·040	0·090	0·124
Curve	[0, 2]	[1, 2]	[2, 2]	[3, 2]

(*b*) and (*d*). $Ro = 0{\cdot}090$. $Re_r/Re\sqrt{\alpha} = -0{\cdot}055$ 0 0·0275 0·055 0·110

Curve	[2, −1]	[2, 0]	[2, 1]	[2, 2]	[2, 3]

the periphery. Thus, the choice of f_{11} has been somewhat arbitrary; however this has had little consequence for the determination of the axial gradient of Γ (see figure 3(*d*)).

Calculated distributions of v_0 and v_{11} (dimensional tangential velocity and gradient), with the effects of varying either the Rossby number or the radial flow level, are shown in figure 3(*a*), (*c*) and figure 3(*b*), (*d*), respectively. The effect

on Γ_{11} (or v_{11}) of varying the Reynolds number Re follows directly from (5) and (6); they are seen to be inversely proportional.

Data for some of the experimental cases on which the calculations have been based are given in table 1.

	No.	μ	r_p cm	Approx. $1/\eta_0$	$2\pi F$ g/sec	v_{p0} cm/sec	Ro	$\sqrt{\alpha}\,\Gamma_{11}(1) = \frac{1}{v_{p0}}\frac{\partial v}{\partial(z/r_p)}$ at $r = r_p$	Ec
Hartnett & Eckert	I	0	3·8	2·5	330	$2{\cdot}4\ 10^4$	0·08	0·027	0·20
Lay, 30 psig	III	0	2·5	3	230	$2{\cdot}9\ 10^4$	0·09	0·024	0·28
Bruun	VII	0·23	4·7	2	120	$1{\cdot}8\ 10^4$	0·03	0·048	0·11
Scheller & Brown	VIII	0·5	1·25	3	14	$2{\cdot}2\ 10^4$	0·04	0·048	0·15
Takahama	IX	0·5	3·9	2·5	60	$2{\cdot}1\ 10^4$	0·02	0·051	0·10
Takahama	X	0·5	2·64	3	60	$1{\cdot}7\ 10^4$	0·05	0·060	0·10

TABLE 1

2.3. *Discussion*

The numerical solution to (5) and (6) is obtained by adjusting f_{00} (a suitable polynomial) until a physically plausible dependence of the circulation $2\pi\Gamma$ on axial position is obtained (see figure 3); thus, the interesting aspect of the solution is on the one hand that a physically plausible axial velocity function (f'_{00}) is created in this way (figure 2(*b*)), on the other hand that very little freedom to vary this arbitrarily is left when all requirements with respect to inflexion, zero points, minimum and integral values are met.

With the shape of f_{00} chosen the magnitude of Γ_{11} (or v_{11}) is found to be almost proportional to Ro^2/Re (cf. figure 3(*c*)). This means that Γ_{11} (or better $\sqrt{\alpha}\,\Gamma_{11}$, which is the relative change in the angular momentum along the axis through a distance equal to the tube radius (see table 1)) is larger the smaller the circulation and the larger the axial volume flow. A comparison with the basic equations (Lewellen 1962) shows the reason to be that the model relates the axial gradient of the centripetal acceleration (v^2/r), through the axial variation of the radial pressure gradient, to turbulent stress created by the radial gradient of the axial velocity.

The Rossby number Ro has the additional influence on Γ that an increase in Ro causes the Γ_0 curve to approach the shape of a free vortex (see figure 3(*a*) where the corresponding v_0 is shown).

With Re in the experimentally interesting range, the shape of Γ_0 is very sensitive to small changes in the radial flow (figure 3(*b*)); the Re_r range covered in the figure corresponds to maximum radial velocities of the order of less than 1 % of the axial velocity. The origin of this effect is, as in the two-dimensional case (see e.g. Keyes 1961 and Ragsdale 1961), a radial influx of angular momentum. When a radial outflow takes place v_0 has a tendency to take on a concave shape (see [2, −1], figure 3(*b*)). A similar effect may be seen in experimental cases; it is caused by a radial outflow of fluid deficient in angular momentum. Analogous results may be obtained within the framework of existing two-dimensional theories.

It is found in the calculations that Γ_{11} is almost unaffected by changes in the radial flow level. Thus, provided the chosen f_{11}-function covers the experimental conditions sufficiently well, it can be concluded (as a comparison with the fundamental equations (Lewellen 1962) shows) that radial transport of axial momentum is of less importance for the axial pressure gradient than turbulent shear stress in the axial direction, at any rate in the outer part of the tube.

It should be noted that the effect on Γ of a radial velocity that increases with ξ is not taken into account in the present approximation, which is limited to linear ψ gradients in the axial direction (see (I) for a discussion of this point).

With Γ_{11} essentially proportional to Ro^2/Re the solution provides a very sensitive means of determining the Re level in any tube for which the geometry, the throughput, and the tangential velocity are all known quantities. The Re values determined in this way contain the apparent turbulent viscosity, which may therefore be extracted; this has been done in (I) in eleven cases from the literature. The turbulent viscosities obtained in this way were of the same order of magnitude as those of previous quasi- two-dimensional studies (Keyes 1961; Ragsdale 1961; Rosenzweig, Lewellen & Ross 1964).

The fundamental inconsistency that the theory is developed for incompressible flow, while the experiments are compressible cases undoubtedly is a serious objection to the quantitative use of the theory. The error introduced by this simplification remains to be estimated. It is felt, however, that the turbulent viscosity estimates, referred to above, together with the test of such results made in § 4 strongly indicate that omission of density changes does not introduce serious order-of-magnitude errors.

3. The total-temperature distribution

3.1. *Theory*

An approximate energy equation pertaining to the flow in typical vortex tubes with turbulence may, according to the analysis by Reynolds (1961) (see also Bruun 1967, 1969) be written

$$\rho u r\,\partial h_0/\partial r + \rho w r\,\partial h_0/\partial z + \overline{\rho' u'} r\,\partial h_0/\partial r + \partial(\rho r \overline{u'h'})/\partial r + \partial(\rho v r \overline{u'v'})/\partial r + \partial(\rho w r \overline{u'w'})/\partial r \simeq 0, \tag{9}$$

where all non-primed symbols refer to mean-time values and primed symbols to fluctuations about the mean; h_0 is the sum of the mean enthalpy and the mean kinetic energy per unit mass (including the mean kinetic energy of the turbulent motion).

An order-of-magnitude analysis for a rather short vortex tube was carried out by Reynolds as follows

$$v \sim O(1), \quad \partial/\partial r \sim O(1), \quad \overline{u'v'} \simeq \overline{u'w'} \sim O(1/100),$$
$$\overline{u'h'} \sim O(1/100) \quad \text{and} \quad \overline{\rho' u'} \sim O(1/100).$$

In order to meet conditions in the main region of the long tubes under consideration here, the following assignments, based on Bruun (1967, 1969) are furthermore made

$$w \sim O(1/5), \quad \partial/\partial z \sim O(1/20) \quad \text{and} \quad u \sim O(1/100).$$

These assignments lead to the conclusion that (9) is quite well approximated by

$$\rho ur\,\partial h_0/\partial r+\rho wr\,\partial h_0/\partial z+\partial(\rho r\overline{u'h'})/\partial r+\partial(\rho vr\overline{u'v'})\,\partial r\simeq 0. \tag{10}$$

Close to the axis with the cold flow fraction large and $v\simeq w$ (see figure 1) this analysis is not strictly valid; however, as mentioned by Reynolds (1961) the error is not likely to play an important part in the overall energy separation.

It is now assumed, following Kassner & Knoernschild (1948) that

$$\overline{u'h'}=-\epsilon_h(\partial h/\partial r-v^2/r) \tag{11}$$

and, following Deissler & Perlmutter (1960) that

$$\overline{u'v'}=-\epsilon(\partial v/\partial r-v/r), \tag{12}$$

where ϵ_h and ϵ are eddy diffusion coefficients for heat and momentum transfer, respectively. Thus, with (11) and (12), equation (10) reads

$$\rho ur\,\partial h_0/\partial r+\rho wr\,\partial h_0/\partial z=(\partial/\partial r)\,[r\rho\epsilon_h(\partial h/\partial r-v^2/r)+r\rho\epsilon(\tfrac{1}{2}\partial v^2/\partial r-v^2/r)]. \tag{13}$$

A similar equation with $\partial h_0/\partial z=0$ was used by Deissler & Perlmutter (1960) for studying the radial temperature gradient. Expression (13) equates the net transport of total-enthalpy, h_0, out of a volume element (left side) with the net accumulation in the volume element of total-enthalpy from radial turbulent diffusion of enthalpy, h, and kinetic energy (right side).

By introduction of the mean total temperature $\tilde{T}\equiv h_0/c_p$ approximated by $T=\tilde{t}+\frac{1}{2}v^2/c_p$, where $\tilde{t}\equiv h/c_p$, on the right side of (13), it becomes

$$\rho ur\,\partial\tilde{T}/\partial r+\rho wr\,\partial\tilde{T}/\partial z=\frac{\partial}{\partial r}[\rho r\epsilon_h(\partial\tilde{T}/\partial r-\partial\tilde{T}_{eq}/\partial r)], \tag{14}$$

with

$$\partial\tilde{T}_{eq}/\partial r\equiv\frac{2}{c_p}\frac{v^2}{r}-\left(\frac{\epsilon}{\epsilon_h}-1\right)\tfrac{1}{2}r^2\frac{\partial(v^2/r^2)}{\partial r}. \tag{15}$$

In the step from (13) to (14), the kinetic energy of both the secondary motion and the turbulent modes is neglected in T on the right side of (13). The error introduced is small, except close to the axis when the cold flow fraction is large.

Now, the axisymmetric stream function, here defined for mass flow,

$$\partial\tilde{\psi}/\partial r\equiv-\rho wr\quad\text{and}\quad\partial\tilde{\psi}/\partial z\equiv\rho ur \tag{16}$$

is introduced together with the angular velocity

$$\tilde{\omega}\equiv v/r. \tag{17}$$

Non-dimensional variables, as defined in § 2 (see equation (4)), are substituted throughout with the change that $2\pi F$ here denotes the total mass flow through the tube, and with the addition that

$$T\equiv\tilde{T}/T_\infty,\quad\partial T_{eq}/\partial r\equiv(1/T_\infty)\,\partial\tilde{T}_{eq}/\partial r\quad\text{and}\quad\omega\equiv\tilde{\omega}/\omega_{p0},$$

T_∞ is the total temperature of the gas entering the tube and $\omega_{p0} = v_{p0}/r_p$ (with v_{p0} the peripheral tangential velocity near the tube nozzle). Equations (14) and (15) then become

$$\frac{\partial\psi}{\partial\xi}\frac{\partial T}{\partial\eta} - \frac{\partial\psi}{\partial\eta}\frac{\partial T}{\partial\xi} = \frac{\partial}{\partial\eta}\left[\frac{2}{Re_h\sqrt{\alpha}}\eta(\partial T/\partial\eta - \partial T_{eq}/\partial\eta)\right], \tag{18}$$

with
$$\partial T_{eq}/\partial\eta = Ec[\omega^2 + \tfrac{1}{2}(1-Pr)\times\eta\,\partial\omega^2/\partial\eta]. \tag{19}$$

Here
$$Re_h \equiv F/(\rho\epsilon_h r_p) \quad \text{and} \quad Ec \equiv v_{p0}^2/(c_p T_\infty) \tag{20}$$

while $\sqrt{\alpha} \equiv r_p/l$, as before, and $Pr \equiv \epsilon/\epsilon_h$. Re_h is a turbulent Reynolds number, essentially axial, Ec an Eckert number, measuring the fraction of available energy converted into kinetic energy, and Pr the turbulent Prandtl number. $\partial T_{eq}/\partial\eta$ is the equilibrium total-temperature gradient which would obtain in the absence of secondary flow.

In search for an approximate solution to (18) it is noted that $\partial T/\partial\xi$ (the axial gradient of total-temperature), according to experiment, may be quite adequately represented by

$$\partial T/\partial\xi = [1 + E(1-\eta)]\,dT_p/d\xi, \tag{21}$$

where $dT_p/d\xi$ is the axial gradient of total temperature at the periphery, i.e. $(\partial T/\partial\xi)_{\eta=1}$, while E is a constant, which has to be determined by some averaging procedure.

In solving the differential equation (18) the method of Cohen (1951) is followed. It is assumed that ψ and ω are known as functions of η and ξ.

As a first step, the total-temperature balance is introduced as follows

$$\int_0^{r_p} \rho w r\tilde{T}\,dr - \int_0^{r_p} \rho\epsilon_h r\,\partial\tilde{T}/\partial z\,dr = \tilde{T}_h\int_0^{r_p}\rho w r\,dr. \tag{22}$$

The equation expresses the fact that the total-enthalpy is preserved in a cylinder (a–a in figure 1 (a)) limited by an arbitrary tube cross-section, the periphery and the hot end of the tube (diffusion into the region from the periphery has been neglected; it is usually small). The second term, the contribution from axial diffusion, is also small under normal conditions. $\tilde{T}_h$ is the total temperature of the hot stream.

In non-dimensional form (22) reads, after partial integration

$$\int_0^1 \psi\,\partial T/\partial\eta\,d\eta - \int_0^1 \frac{\sqrt{\alpha}}{2Re_h}\,\partial T/\partial\xi\,d\eta = \psi_h(T_p - T_h), \tag{23}$$

where $-\psi_h = 1-\mu$ is the hot flow fraction.

By aid of (21) an explicit expression for $\partial T/\partial\eta$ is readily obtained from (18), which with ξ constant is a first-order differential equation in $\eta\,\partial T/\partial\eta$, as follows

$$\eta\frac{\partial T}{\partial\eta} = \phi(\eta)\left[\int_0^\eta \frac{1}{\phi(\eta')}\left(-\tfrac{1}{2}Re_h\sqrt{\alpha}\frac{\partial\psi}{\partial\eta'}\frac{\partial T}{\partial\xi} + \frac{\partial}{\partial\eta'}\left(\eta'\frac{\partial T_{eq}}{\partial\eta'}\right)\right)d\eta'\right], \tag{24}$$

where
$$\phi(\eta) \equiv \exp\left\{\int_0^\eta Re_h\sqrt{\alpha}/(2\eta')\times\partial\psi/\partial\xi\,d\eta'\right\} \tag{25}$$

and where the boundary condition $(\eta\,\partial T/\partial\eta)_{\eta=0} = 0$ has been used.

This solution to (18) is inserted into the enthalpy balance equation (23) to yield a first-order differential equation in T_p or $T_p - T_h$:

$$d(T_p - T_h)/d\xi = -\frac{\psi_h}{c_5}(T_p - T_h) + \frac{c_1}{c_5}. \tag{26}$$

Here $c_5 \equiv c_2 + c_3$ with

$$c_3 \equiv \int_0^1 \psi \left[\frac{\phi}{\eta}\int_0^\eta \frac{Re_h\sqrt{\alpha}}{2\phi}\frac{\partial\psi}{\partial\eta'}(1+E(1-\eta'))\,d\eta'\right]d\eta \tag{27}$$

and

$$c_2 \equiv \int_0^1 \frac{\sqrt{\alpha}}{2Re_h}(1+E(1-\eta))\,d\eta \tag{28}$$

(where normally c_2 may be neglected), while

$$c_1 \equiv \int_0^1 \psi \left[\frac{\phi}{\eta}\int_0^\eta \frac{1}{\phi}\frac{\partial}{\partial\eta'}(\eta'\,\partial T_{eq}/\partial\eta')\,d\eta'\right]d\eta \tag{29}$$

with $\partial T_{eq}/\partial\eta$ as defined in (19).

A formal solution to (26) is readily obtained, yielding an expression for $T_p - T_h$ with one integration constant to be determined.

The solution also determines $dT_p/d\xi$ and, through (21), $\partial T/\partial\xi$. Thus $\partial T/\partial\eta$ may be calculated on the basis of (24):

$$T - T_h = T_p - T_h + \int_1^\eta \partial T/\partial\eta'\,d\eta'. \tag{30}$$

When this equation is differentiated with respect to ξ an expression for $\partial T/\partial\xi$ is obtained as follows

$$\frac{\partial T}{\partial\xi} = \frac{dT_p}{d\xi} + \int_1^\eta \frac{\partial^2 T}{\partial\eta'\,\partial\xi}d\eta'. \tag{31}$$

Equations (21) and (31) represent two alternative expressions for $\partial T/\partial\xi$. These have to be matched as well as possible by the selection of an optimal E value. Since to a first approximation

$$\int_1^\eta \frac{\partial^2 T}{\partial\eta'\,\partial\xi}d\eta' = (\eta - 1)\frac{\overline{\partial^2 T}}{\partial\eta\,\partial\xi},$$

it appeared reasonable to demand, for this purpose, that

$$\frac{dT_p}{d\xi}E(1-\eta) = -(1-\eta)\frac{\overline{\partial^2 T}}{\partial\eta\,\partial\xi} \quad \text{where} \quad \frac{\overline{\partial^2 T}}{\partial\eta\,\partial\xi} \equiv \int_0^1 \frac{\partial}{\partial\xi}\left(\frac{\partial T}{\partial\eta}\right)d\eta \tag{32}$$

with $\partial T/\partial\eta$ determined according to (24); this choice is seen to make (31) identical with (21) at both $\eta = 1$ and 0. Furthermore, as E according to its definition is independent of ξ, it was necessary to average over this co-ordinate as well, thus

$$\bar{E} = -\frac{\int_0^1 \left[\left(\frac{\partial T}{\partial\eta}\right)_{\xi=1} - \left(\frac{\partial T}{\partial\eta}\right)_{\xi=0}\right]d\eta}{T_p(1) - T_p(0)}. \tag{33}$$

The second averaging procedure introduces, in most cases of interest, only a minor mathematical inconsistency. $\bar{E}$ must be found by iteration.

Two parameters, the absolute temperature level and the integration constant in the solution to equation (26) remain to be fixed. The first is determined so that the mean total-temperature of the gas entering the annulus between $\eta = \eta_0$ and $\eta = 1$ (see figure 1(*b*)) at $\xi = 0$ is equal to that of the gas in the inlet nozzle (assuming little or no gas to escape directly to the cold exit), thus

$$\left[\int_{\eta_0}^{1} (1-T)\,\partial\psi/\partial\eta\,d\eta\right]_{\xi=0} = 0. \tag{34}$$

The integration constant is determined through the parameter

$$\Delta T_h \equiv (T_p - T_h)_{\xi=1}$$

and by reference to experiment.

It may be useful to illustrate the type of solution to the partial differential equation obtained here, by a simple example. For that purpose, it is assumed that both ψ and ω are independent of ξ, and that the Prandtl number $Pr = 1$; then (24) reduces to

$$\frac{\partial T}{\partial \eta} = -\frac{Re_h\sqrt{\alpha}}{2\eta}\int_0^{\eta} \frac{\partial\psi}{\partial\eta'}\frac{\partial T}{\partial\xi}\,d\eta' + Ec\times\omega^2 \tag{35}$$

and (27) to

$$c_5 \simeq c_3 = \frac{Re_h\sqrt{\alpha}}{2}\int_0^1 \frac{\psi}{\eta}\left[\int_0^{\eta}\frac{\partial\psi}{\partial\eta'}(1+\bar{E}(1-\eta'))\,d\eta'\right]d\eta, \tag{36}$$

while

$$c_1 = Ec\int_0^1 \psi\omega^2\,d\eta. \tag{37}$$

As both c_1 and c_5 are independent of ξ in this simple case, the solution to the differential equation (26) is

$$T_p - T_h = C\times\exp\{-\psi_h\,\xi/c_5\} + c_1/\psi_h, \tag{38}$$

where C is the integration constant; when $\Delta T_h = 0$

$$T_p - T_h = [1-\exp\{(1-\xi)\,\psi_h/c_5\}]\,c_1/\psi_h, \tag{39}$$

i.e. T_p is here a simple exponential function in ξ.

It should be emphasized that the solution to the partial differential equation (18) represented by (24) to (29)—or in the simple case, (35) to (39)—leaves no possibility of specifying the radial temperature distributions at the axial boundaries in any detail, nor the temperature gradient at the periphery. Furthermore, the solution is of physical relevance only to the extent that the axial temperature gradient is reasonably well represented by (21). However, when agreement is attained, the solution provides a simple link between the flow field and the energy distribution within the tube excluding all boundary layers. In Linderstrøm-Lang (1970*b*) (referred to below as (II)) these points are further discussed.

The methods used in the computations are outlined in (II). The secondary stream function (ψ) and the tangential velocity function employed in the calculations are chosen among the sets devised and calculated, respectively, in the work on the velocity distribution (see § 2).

3.2. *Counter-flow analogies*

Flow in typical counter-flow systems is shown in figure 4(*a*) and (*b*), where (*a*) refers to a distillation column and (*b*) to a heat exchanger or an extraction column. N is the dependent variable, i.e. the concentration or the temperature;

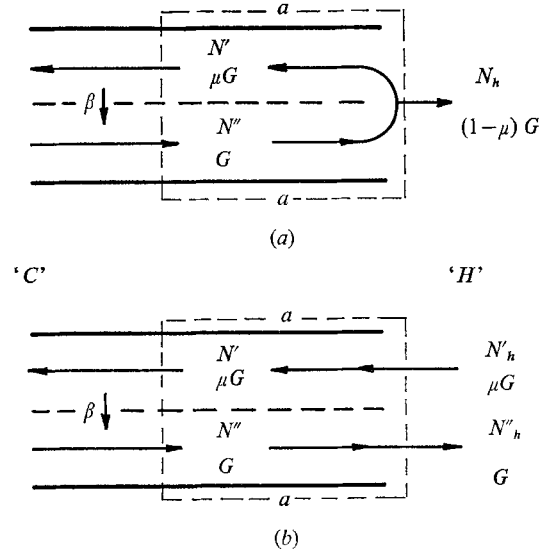

FIGURE 4. Diagrams of counter-current systems. (*a*) Distillation column; (*b*) heat exchanger or extraction column.

G and μG are the mass flow rates in the two streams; β represents a transverse 'force', the presence of which results in $N''-N' \neq 0$ at equilibrium; one may write

$$G\,dN''/dz = -K[(N''-N')-\beta], \tag{40}$$

where K is a factor that measures the specific rate of either mass-component transport or heat transport by diffusion, across the boundary between the two streams. β is zero in a heat exchanger.

The thermal, or mass component, balance equation over the section of the column or exchanger limited by *a*–*a* in figure 4 is written

$$N'' = N'\mu + (1-\mu)\,\bar{N}_h, \tag{41}$$

where, in case of figure 4(*b*),

$$\bar{N}_h = 1/(1-\mu)\,(N''_h - \mu N'_h).$$

Equations (40) and (41) combined give a differential equation that determines the concentration or the temperature change along the column or exchanger

$$\frac{dN''}{dz} = \frac{K}{G}\frac{1-\mu}{\mu}(N''-\bar{N}_h) + \frac{K}{G}\beta. \tag{42}$$

The flow in the vortex tube is in principle (according to the present model) as shown in figure 4(*a*); furthermore (40)–(42) correspond closely to (18), (23), and (26) with β determined by the radial pressure gradient. Thus it is possible to write (equations (29) and (27))

$$c_1 = \mu\beta \quad \text{and} \quad c_5 = \mu G/K. \tag{43}$$

It is seen (figure 4) that c_1, in the mass separator case, is the product of the fraction of gas moving left (towards the 'cold end') and the factor β which measures the equilibrium condition. In the present case c_1 is in principle the same applied to total-enthalpy, but it is also a complex function of ψ (the secondary flow function) that takes into account the effect of the interplay between axial flow and driving force (pressure gradient) on the peripheral total-temperature change.

In the mass separator (heat exchanger) case c_5 is the mass flow towards the left (the 'cold' flow) divided by the specific rate of heat or mass-component transfer across the stream boundary. In the present case it is a similar parameter; however, at the same time it is a complicated function of ψ that takes into account the influence of the shape (but not absolute magnitude) of the radial and axial total-temperature gradients on the temperature change at the periphery. $-\psi_h \equiv 1-\mu$ is in all cases the net mass flow fraction through the 'hot exit', to the right.

The presence of the term c_1 in the governing differential equations is as essential for successful chemical separation in distillation columns (figure 4(*a*)) as it is for H the total-enthalpy separation in the vortex tube.

3.3. *Results, parameter study*

The mathematical accuracy of the solutions to the partial differential equation (18) obtained according to the method described in the previous sections may, as discussed in (II), be tested through a comparison of $\partial T/\partial\xi$ from (31) (with $\partial T/\partial\eta$ determined according to (24)) with that from (21). In cases where $\partial T/\partial\xi$ is large compared to $\partial T/\partial\eta$, as happens at high cold flow fraction (see below), the mathematical argument leading from (23) to (26) directly implies that the error introduced by replacing $\partial T/\partial\xi$ by a linear function in η, as is here done, is small.

Parameters. The pertinent parameters for the description of the total-temperature distribution according to the present model are the Eckert number, Ec; the Prandtl number, Pr; the cold flow fraction, μ; the ratio of radial to axial mass flow, $Re_{hr}/(\sqrt{\alpha}\, Re_h)$ (see equation (8), § 2 and (II)); the Reynolds number, Re_h; and the boundary parameter ΔT_h, which fixes the total-temperature distribution at $\xi = 1$ relative to the temperature of the hot stream.

In addition to the above parameters, the E parameter, which determines the radial gradient of $\partial T/\partial\xi$, is of primary importance for the discussion, as it is imperative that the optimal E values selected according to equation (33) lead to solutions with boundary functions that approximate those of real vortex tubes; a discussion of these problems is presented in (II). In all instances tested, E values, quite closely correlated with experiment, have in fact been found. Furthermore, a meaningful comparison may be made, even though the set of boundary conditions derived in the calculations does not exactly match those of the experiments.

The Eckert number. The effect of an increase of Ec by some factor is an increase of both $\partial T/\partial\eta$ and $\partial T/\partial\xi$ by the same factor (equations (18) and (23) taking into consideration that Ec cancels in the calculation of $\bar{E}$). It is clear, therefore, that the Ec value has no qualitative influence on the results; it is a quantitative

measure of the kinetic energy of the gas, and in that capacity it governs the absolute level of the total-temperature separation potential of the tube.

The Prandtl number. Pr, or rather its deviation from unity, has a modifying influence on the radial temperature gradients mainly at the periphery where $\partial\omega^2/\partial\eta$ (equation (19)) usually is numerically large and negative (see figure 10(*a*)). According to Shapiro (1954), a turbulent Prandtl number of 0·7 is indicated experimentally; on the other hand a Prandtl number of unity has often been assumed. The concept, as such, has a weak theoretical basis, and there is probably little to distinguish between the two possibilities. Fortunately, the effect on the present results is unimportant (cf. figure 10(*a*)). It should be added, that the treatment here is based on the assumption, first made by Kassner & Knoernschild, that the turbulent motion of a lump of fluid in the radial pressure gradient is adiabatic. This may not be entirely true, in which case the term $Ec\omega^2$ in equation (19) is reduced in magnitude.

The cold flow fraction. The influence of μ on the total-temperature distribution in the vortex tube is of major importance. The reason is obvious when reference is made to the heat exchanger (or distillation column) analogy. When μ, the fraction of cold gas, is small any large increase in total temperature with ξ, in the stream flowing in the core towards the cold exit, will lead to only a small total-temperature increase with ξ in the outer stream (compare figures 1 and 4). A small amount of the net total enthalpy transport across the η_0 boundary can cause the change, and a total-temperature distribution close to what may be termed the pseudo-equilibrium distribution, as determined by the radial flow (see below for a definition of this term) can be easily established and maintained along the tube; see figure 9 for a typical example. The performance of the tube as a total-enthalpy separator is under these conditions poor.

When the cold flow fraction is increased, an increasing amount of total-enthalpy will have to diffuse from the cold stream to the hot in order to change the temperature of the former. Non-equilibrium conditions with the radial temperature gradient rather flat at intermediate ξ-values and even at low ξ become more probable, with the result that a substantial amount of total enthalpy passes the boundary between the two streams. Thus, an axial gradient of total-temperature is established at all radii, though largest in the core (see figures 5, 10 and 11 for typical examples). The function of the tube as a total-enthalpy separator has improved.

When the cold stream becomes substantial as μ passes a value of $\frac{1}{2}$, the temperature change with ξ in the two streams approach one another. Any non-equilibrium distribution at $\xi = 1$ therefore tends to prevail at all ξ. The diffusion across the boundary will lead to a large axial total-temperature gradient, which may well be larger than the radial temperature gradient (see figure 12 for a typical example). The tube is likely to function well as a total-enthalpy separator.

When the cold flow fraction goes to one, the amount of total enthalpy transferred radially may well continue to increase but, as most of the gas is returned in the core, the net amount goes to zero. At the same time the axial temperature change approaches a maximum, the value of which is easily found in the simple

case where ψ and Γ are independent of ξ (equations(35) to (39)). Equation (39) directly gives the limiting value as

$$T_p(1)-T_p(0)\,(=-T_p(0)+T_h)=-(1-\exp\{\psi_h/c_5\})\,c_1/\psi_h \to c_1/c_5. \qquad (44)$$

The radial flow (or Re_{hr}). The radial flow acts through the term $(\partial\psi/\partial\xi)(\partial T/\partial\eta)$ in equation (18) as a kind of net diffusion term which counteracts, in the case of inflow, the effect of the pressure gradient with the result that the apparent equilibrium gradient on the average is smaller than $\partial T_{eq}/\partial\eta$ (see figure 5). The

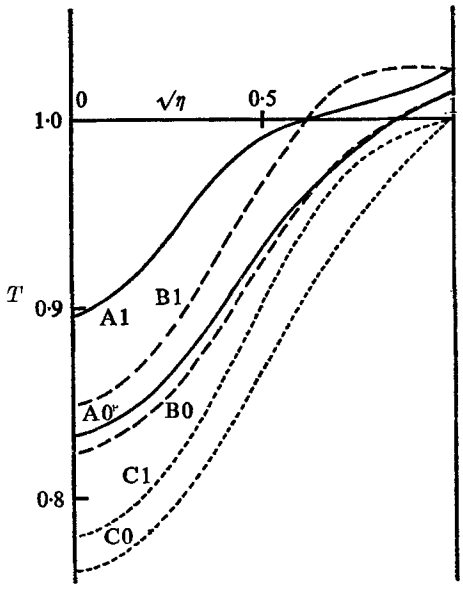

FIGURE 5. Non-dimensional total-temperature T $(=\tilde{T}/T_\infty)$ as a function of non-dimensional radius $\sqrt{\eta}$ $(=r/r_p)$ (A curves); with pseudo-equilibrium distribution, referred to peripheral total temperature T_p for convenience (B curves); and equilibrium distribution, $\int_1^\eta (\partial T_{eq}/\partial\eta')\,d\eta'$, plus 1 for convenience (C curves); at axial positions $\xi\,(=z/l)=0$ and 1. Data as in table 2.

effect of varying Re_{hr}/Re_h is shown in figure 8 for $\mu = 0{\cdot}23$; the radial flow reduces both the radial and the axial total-temperature gradients. The effect increases with decreasing cold flow fraction and dominates conditions at $\mu = 0$ (see below).

The Reynolds number. Re_h is a measure of the relative importance of the total-enthalpy transport by secondary flow and by turbulent diffusion. As such it is a measure of the effect of both the radial and the axial flow (through equations (24) and (25)) on the total-enthalpy separation. Thus, when Re_h goes to zero because the secondary flow decreases relative to the turbulent diffusion, the equilibrium distribution $\partial T_{eq}/\partial\eta$ is approached at all η and ξ (18) or (24) as far as permitted by the axial diffusion represented by c_2, (28). Conversely, when Re_h goes to infinity and the secondary flow becomes of dominating importance, the diffusion term in equation (18) may be neglected, and there will be hardly any total-temperature change in the tube.

Figure	Case	Cold flow fraction	Eckert number $Ec = \frac{v_{p0}^2}{c_p T_\infty}$ (equation (20))	Turb. Prandtl number Pr	Turb. Reynolds number $\sqrt{\alpha} Re_h = \frac{F}{\rho \epsilon_h r_p}$ (equation (20))	Radial turb. Reynolds number Re_{hr}	Ratio of radial flow to total flow $Re_{hr}/\sqrt{\alpha}\, Re_h$ (equation (8))	Relative axial grad. of circulation $(\Gamma_{11})_{\eta=1} = \frac{l}{v_{p0}} \left(\frac{\partial v}{\partial z}\right)_{\eta=1}$ (equation (8))	$\Delta T_h = T_p(1) - T_h$	$\sqrt{\eta_0} = \frac{r_0}{r_p}$ (figure 1)	$\bar{E}$ (equation (33))
5	495	0·23	0·11	0·7	6·2	1·0	0·16	−0·38	0	0·63	2·20
6	495	0·23	0·11	0·7	6·2	1·0	0·16	0·0/−0·76	0	0·63	0·36/2.60
7	495	0·23	0·11	0·7	3·1/9·3	1·0	0·16	−0·38	0	0·63	1·56/3·40
8	495	0·23	0·11	0·7	6·2	0·0/2·0	0·0/0·32	−0·38	0	0·63	5·4/2·6
9(*a*)	392	0·02	0·14	1·0	20	2·4	0·12	−0·45	0	0·58	−1·38
10(*a*)	495	0·23	0·092	0·7/1·0	7·0	1·12	0·16	−0·38	0	0·63	2·24/1·76
11(*a*)	480	0·49	0·092	0·7	3·5	0·35	0·10	−0·57	0·01/0·0	0·63	0·92/0·98
12(*a*)	497	0·76	0·092	0·7	7·0/3·5	2·4	0·34/0·68	−0·45	0	0·63	0·36/0·27
13(*a*)	480	0·49	0·092	0·7	3·5	0·35	0·10	−0·57	0·01	0·63	0·92
14(*a*)	—	—	0·092	0·7	3·5	0·70	0·20	−0·45	—	—	—

TABLE 2

The effect of Re_h is very slight when the cold flow fraction, μ, is low, because (pseudo-) equilibrium is attained at almost all ξ, while at $\mu = 0{\cdot}25$ the over-all effect is a reduction of the axial total-temperature gradient with increasing Re_h (figure 7). Note that, at small Re_h (in figure 7), the axial total-temperature gradient becomes non-linear in ξ, because pseudo-equilibrium is more rapidly approached under these conditions. At high μ the axial gradient becomes almost inversely proportional to Re_h (see figure 12) in agreement with expression (44), which contains Re_h in c_5 of the denominator.

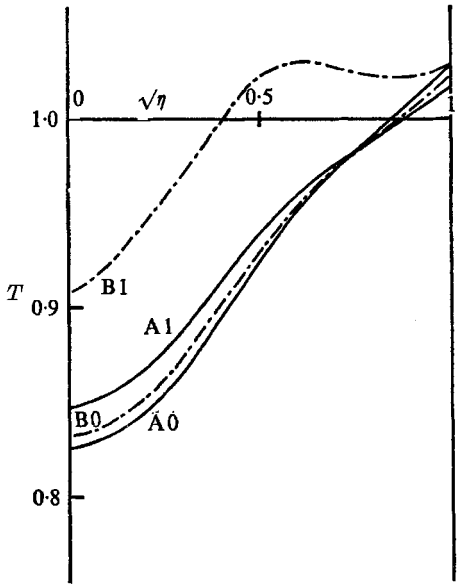

FIGURE 6

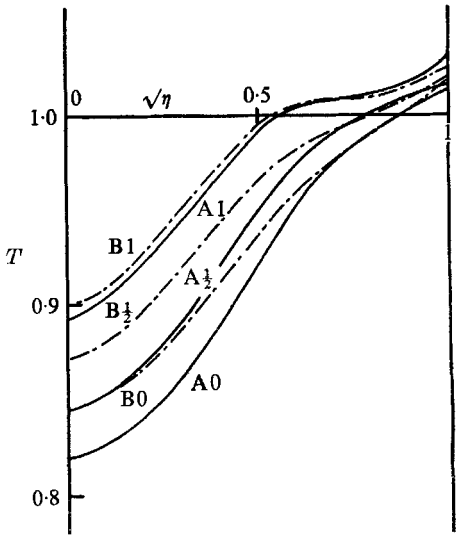

FIGURE 7

FIGURE 6. Influence of axial gradient of angular velocity (or Γ_{11}). Total-temperature as a function of radius at $\xi = 0$ and $\xi = 1$. Case 495; input data as in figure 5 (see table 2), except: A curves, $\Gamma_{11} = 0$; B curves, $(\Gamma_{11})_{\eta=1} = -0{\cdot}76$.

FIGURE 7. Influence of Reynolds number. Total temperature as a function of radius at $\xi = 0$, $\frac{1}{2}$ and 1. Case 495; input data as in figure 5 (see table 2) except: A curves, $Re_h\sqrt{\alpha} = 3{\cdot}1$; B curves, $Re_h\sqrt{\alpha} = 9.3$.

Besides the above parameters, the shape of the tangential velocity pattern is of importance to the total-temperature distribution. Thus, the equilibrium total-temperature gradient, $\partial T_{eq}/\partial\eta$, is very sensitive to changes in the radial distribution of the tangential velocity, i.e. v_0, while the axial tangential velocity gradient v_{11}—because it leads to a decrease in $\partial T_{eq}/\partial\eta$ with axial position—may produce noticeable axial total temperature gradients (at any rate at low μ), see figure 6 (where, admittedly, part of the effect may be mathematical rather than physical).

3.4. *Comparison with experiment*

Most experiments pertain to cases where the cold flow fraction has been zero. As explained above, the distribution is likely under these conditions to be the essentially two-dimensional distribution assumed by previous workers (Deissler

& Perlmutter 1960; Hartnett & Eckert 1957; Takahama 1965); any axial gradient of total temperature is then caused by the axial decay of ω (compare figure 6).

Figure 9 (*a*) is an attempt to approximate the experimental distribution shown in figure 9 (*b*). The *Ec* value employed for the calculated case is the one that leads to the experimental overall equilibrium temperature difference,

$$\int_0^1 \partial T_{eq}/\partial\eta \, d\eta,$$

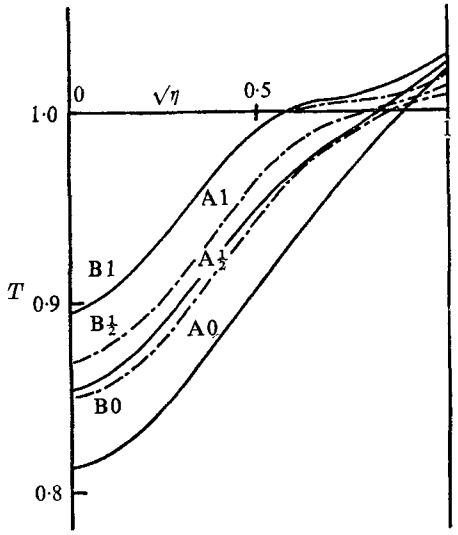

FIGURE 8. Influence of radial flow. Total temperature as a function of radius at $\xi = 0, \frac{1}{2}$ and 1 Case 495; input data as in figure 5 (see table 2), except: $Re_{hr}/Re_h\sqrt{\alpha}$ (A curves) = 0, (B curves) = 0·32.

as indicated by the dashed lines; the Re_h and Re_{hr} used are derived from the velocity study. The fit is by no means perfect at low η, especially close to $\xi = 1$. However, one feature that is well reproduced is the axial total-temperature gradient at the periphery, $\partial T_p/d\xi$, which comes out negative both in calculations and experiments. The reason for this cross-over phenomenon is, according to the model, that the outer part of the tube in this case acts as a concurrent system (see discussion in (II)).

There are two obvious reasons for the discrepancy between figure 9 (*a*) and (*b*). Either the axial boundary conditions at $\xi = 1$ are not identical in the two cases, and the agreement at lower ξ values is attained because the experimental system quickly adjusts to the quasi-equilibrium condition. Or, the radial inflow is not constant but increases with axial position, so that the quasi-equilibrium gradient becomes less steep with ξ. The present model does not permit a demonstration of this effect, as it is limited to ψ functions that are linear in ξ.

$\mu = 0{\cdot}23$. The conditions are rather different at this cold flow fraction. The model calculations show that the axial temperature gradient accounts for the major part of the diffusion term in equation (18), except near $\xi = 0$ where the

pseudo-equilibrium gradient obtains (see figure 5). In figure 10, a comparison with experiment is carried out; Re_h is taken from § 4, while Re_{hr}/Re_h is derived from experiment. The correlation is quite satisfactory, though the radial gradient definitely is too steep at low η.

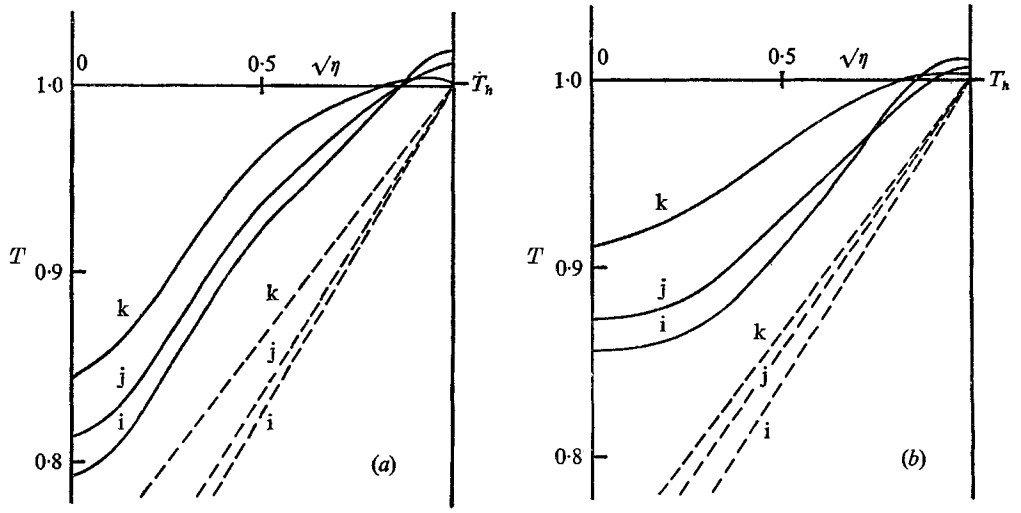

FIGURE 9. Comparison of calculated and experimental total-temperature distributions at cold flow fraction $\mu \simeq 0$, for $\xi = 0{\cdot}06$ (i), $\xi = 0{\cdot}34$ (j), and $\xi = 1{\cdot}0$ (k). Ec_{calc} chosen to give same average equilibrium total-temperature gradients (dashed lines) in figures (*a*) and (*b*). Ratio of radius to length of region I (figure 1) $\sqrt{\alpha}$ $(= r_p/l) = 1/12$, $Pr = 1$. (*a*) Case 392; data as in table 2. (*b*) Case I, Hartnett & Eckert; data as in table 1.

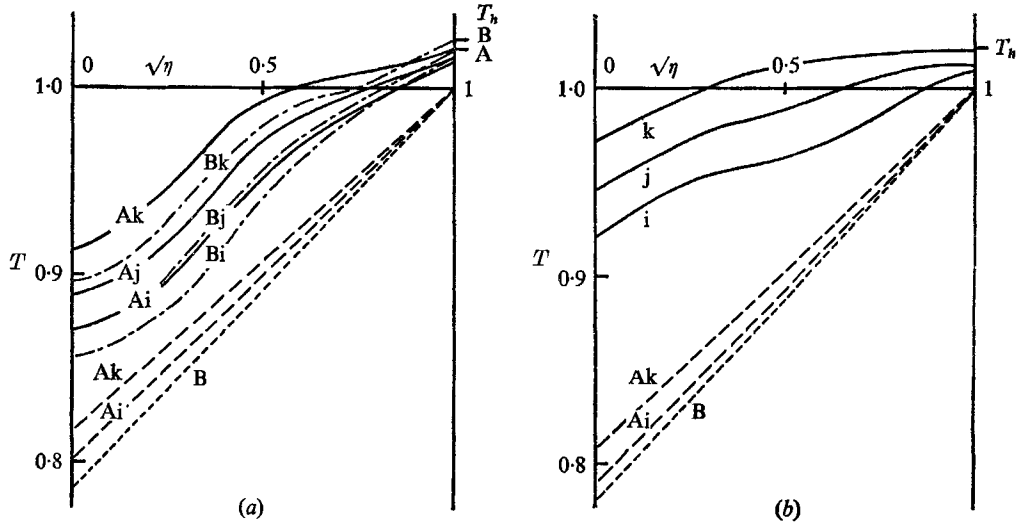

FIGURE 10. Comparison of calculated and experimental total-temperature distributions at $\mu = 0{\cdot}23$ for $\xi = 0{\cdot}15$ (i), $\xi = 0{\cdot}53$ (j), and $\xi = 1{\cdot}0$ (k). Dashed straight lines indicate average equilibrium total-temperature gradients. $\sqrt{\alpha} = 1/10{\cdot}4$. (*a*) Case 495; A curves $Pr = 0{\cdot}7$, B curves $Pr = 1$; Ec determined as in figure 9(*a*); data as in table 2. (*b*) Case VII, Bruun; data as in table 1.

$\mu = 0{\cdot}5$. At this cold flow fraction the tube approaches optimal operation as a total-enthalpy separator, and $\partial T/\partial \xi$ is quite appreciable. In figure 11 (*b*), an experimental case is shown that may be somewhat atypical in that the gas moving into the central region at $\xi = 1$ has a higher total temperature than the gas moving in the other direction in the outer annulus. Under normal conditions motion towards the centre, accompanied by a flow reversal, as must take place to some extent beyond region I (i.e. in region IV of figure 1), will lead to a lowered total temperature, as also happens in analogous experiments by Takahama & Kawashima (1960). It is tempting to relate the 'anomalous' effect in figure 11 (*b*) to the occurrence of a 'vortex breakdown' (Benjamin 1962) or to a 'hot spot' (Stone & Love 1950) in region IV.

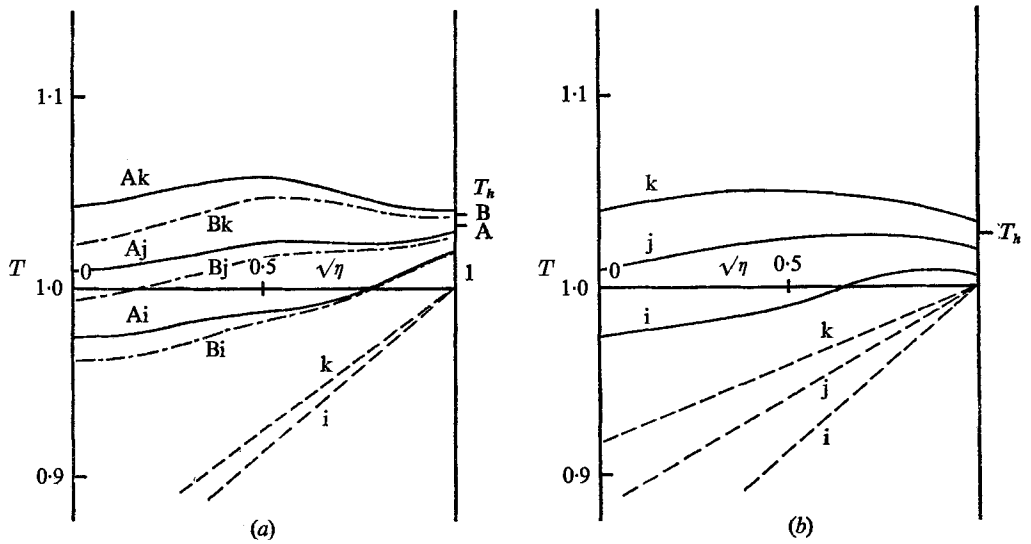

FIGURE 11. Comparison of calculated and experimental total-temperature distributions at $\mu = 0{\cdot}49$ for $\xi = 0{\cdot}17$ (i), $\xi = 0{\cdot}59$ (j), and $\xi = 1{\cdot}0$ (k). Dashed straight lines indicate average equilibrium total-temperature gradients. $\sqrt{\alpha} = 1/14{\cdot}5$, $Pr = 0{\cdot}7$. (*a*) Case 480; A curves $\Delta T_h = 0{\cdot}01$; B curves $\Delta T_h = 0$. *Ec* determined as in figure 9 (*a*); data as in table 2. (*b*) Case VIII, Scheller & Brown; data as in table 1.

It is seen from figure 11 (*a*) that adjustment of the ΔT_h parameter to the experimental $T_p(1) - T_h$ value leads to a satisfactory reproduction of the experimental distribution in figure 11 (*b*). It is worth noting that the Re_h value employed is the best value according to the results in § 4.

$\mu = 0{\cdot}76$. No experimental T values at this cut have been available to the author; however Suzuki (1960) provides some velocity data at $\mu = 1$, which are helpful in the choice of an appropriate tangential velocity distribution (figure 12 (*b*)). Figure 12 (*a*) shows a calculated temperature distribution. $\partial T/\partial \xi$ is now large compared to $\partial T/\partial \eta$ and, as discussed already, Re_h has a major influence on the axial temperature gradient.

The total-enthalpy separation is caused by turbulent transport of both heat and kinetic energy. Figure 13 gives an impression of the relative importance of the two contributions: the larger the difference is between the slopes of two

corresponding A and B curves at a given η value, the stronger the diffusion current. Thus, it may be deduced by a comparison of figures 13 (*a*) and (*b*) that the kinetic energy diffusion contributes most to the total-temperature separation at radii close to the periphery, while heat diffusion dominates near the centre axis; a conclusion also reached by Reynolds (1961). The results in figure 13 indicate that

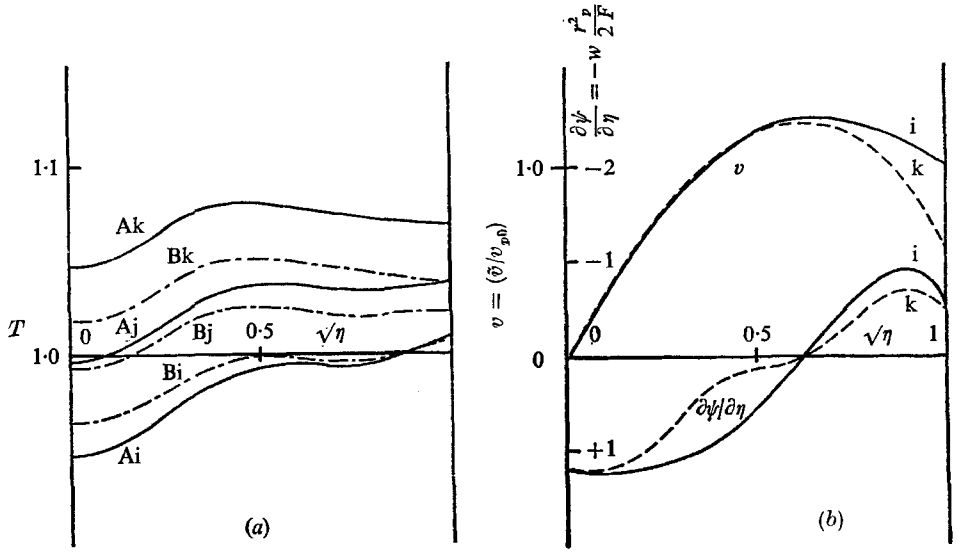

FIGURE 12. $\mu = 0{\cdot}76$. (*a*) Calculated total-temperature distribution at $\xi = 0$ (i), $\frac{1}{2}$ (j) and 1 (k). A curves, $Re_h\sqrt{\alpha} = 7$; B curves, $Re_h\sqrt{\alpha} = 3{\cdot}5$. Data as in table 2. (*b*) Corresponding secondary flow ($Re_{hr}/(Re_h\sqrt{\alpha}) = 0{\cdot}34$) and tangential velocity distributions; see § 2.

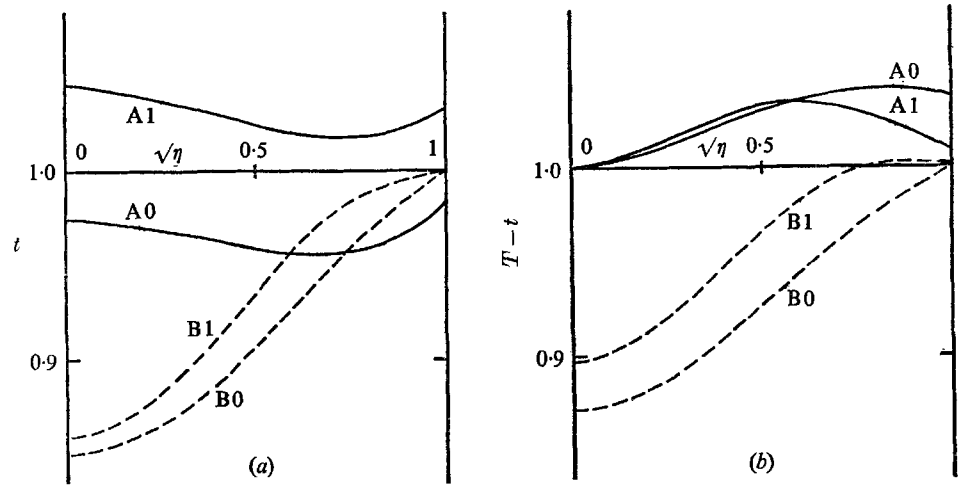

FIGURE 13. (*a*) Calculated non-dimensional static temperature $t\ (= \bar{t}/T_\infty)$ as a function of radius (A curves); with equilibrium (adiabatic) static temperature distribution, referred to 1·0 at $\eta = 1$ for convenience (B curves); at $\xi = 0$ and $\xi = 1$. (*b*) Difference between calculated total- and static-temperatures ($T - t$) as a function of radius (A curves) with equilibrium curves (B) referred to 1·0 at $\eta = 1$ for convenience; at $\xi = 0$ and $\xi = 1$. Case 480; data as in figure 11 (*a*), $\Delta T_h = 0{\cdot}01$ (see table 2).

the axial decay of tangential velocity in the outer part of the tube may at high ξ lead to an enhanced outward transport of kinetic energy that is partly compensated by an inward transport of heat.

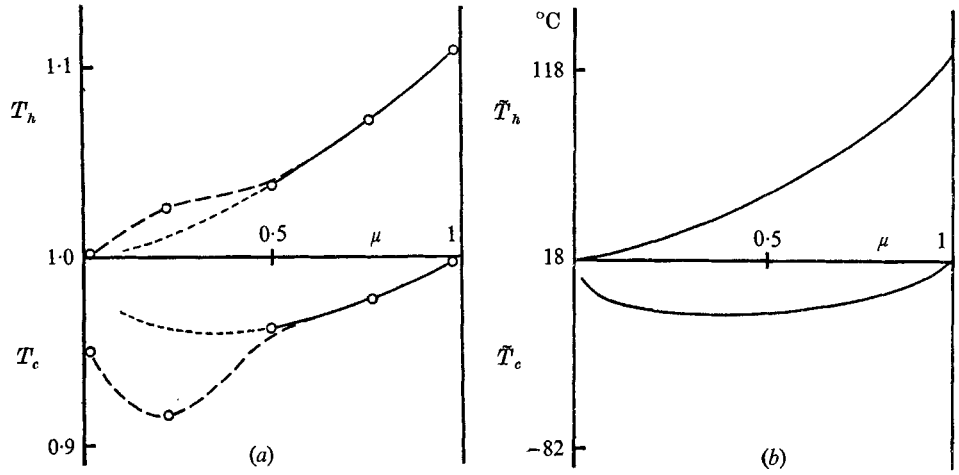

FIGURE 14. Temperature separation as a function of cold flow fraction, μ. (*a*) Calculated curve, data as in table 2. (*b*) Data from Hilsch (1946).

The overall temperature separation as calculated from the above examples is compared with experiment in figure 14. At high μ the trend should be realistic; thus, the upward concave tendency of both curves is readily explained by the theory. A close fit with experiment at low cold flow fraction is, however, not to be expected as the influence of the (poorly defined) radial flow and that of uncertain axial boundary conditions have been shown above to be rather great under these conditions. Only the typical decreasing performance of vortex tubes as μ approaches zero is reproduced quite well in figure 14(*a*). This is achieved by permitting a central flow into the tube proper through the cold end orifice. Such reversed flow on the axis is known to exist when $\mu = 0$ and it is likely to persist at μ somewhat greater than zero. If the net flow out of the cold exit is small enough compared to the total flow in the duct, the cold stream temperature will rise to close to the inlet temperature, so that a small, or vanishing, net temperature difference is the result.

4. Performance

4.1. *The value increase*

By analogy with a procedure adopted in case of mass separation (Cohen 1951) the performance of a vortex tube is equated to a 'value increase' that the gas is said to experience while passing through the tube; i.e. it is assumed that any stream of gas has a value, A, which is the product of a specific value-function, V, and the amount, G, of gas in the stream; where V is some function of the total-temperature of the stream to be determined later (equations (52), (53)). The 'value increase' over the vortex tube is then (with normalized total-temperatures)

$$\Delta A \equiv 2\pi F[\mu V(T_c) + (1-\mu)\, V(T_h) - V(1)], \tag{45}$$

while the infinitesimal value-increase over a volume element in the tube is

$$dA = \oint_{\sigma} V(T)\,\delta\mathbf{G}\,d\boldsymbol{\sigma}, \tag{46}$$

where the integration is over the surface of the volume element and $\delta\mathbf{G}\,d\boldsymbol{\sigma}$ is the mass flow normal to and through the surface $d\sigma$, i.e.

$$\oint_{\sigma} \delta\mathbf{G}\,d\boldsymbol{\sigma} = 0. \tag{47}$$

The integral of dA over any finite region of the tube

$$\Delta A = \iiint dA \tag{48}$$

is seen to be the net value-increase over the region. When the whole tube is considered, (48) becomes identical with (45).

Expansion of $V(T)$ in (46) in a Taylor series about a fixed point of total temperature T^* within the volume element, and use of (47), lead to

$$dA = (dV/dT)_{T^*} \oint_{\sigma} T\,\delta\mathbf{G}\,d\boldsymbol{\sigma}. \tag{49}$$

The integrand to the right is seen to be the net transport of total-enthalpy (divided by T_∞) out of the volume element by secondary flow; thus, according to (14) or (18) in the previous section, and with the introduction of non-dimensional quantities throughout,

$$\frac{dA}{2\pi F} = \frac{1}{2\pi}\frac{dV}{dT}\frac{\partial}{\partial\eta}\left(\frac{2\eta}{Re_h\sqrt{\alpha}}\left(\frac{\partial T}{\partial\eta} - \frac{\partial T_{eq}}{\partial\eta}\right)\right) d\eta\,d\xi\,d\theta. \tag{50}$$

Insertion of this expression into (48) referred to the whole of region I, figure 1, and partial integration lead to

$$\frac{\Delta A}{2\pi F} = d_p - \int_0^1\int_0^1 \frac{d^2V}{dT^2}\frac{2}{Re_h\sqrt{\alpha}}\frac{\partial T}{\partial\eta}\,\eta\left(\frac{\partial T}{\partial\eta} - \frac{\partial T_{eq}}{\partial\eta}\right) d\xi\,d\eta \tag{51}$$

(with the integration over the angular co-ordinate carried out). d_p is a measure of the value-change due to diffusion through the peripheral wall; experiments have shown this contribution to the functioning of the tube to be unimportant; consequently the term will be neglected.

Expression (51) is valid regardless of the form chosen for the specific value-function V; the simplest choice possible is therefore made, i.e.

$$d^2V/dT^2 \equiv 1, \tag{52}$$

which integrated twice and with suitable integration constants gives

$$V = \tfrac{1}{2}(T-1)^2. \tag{53}$$

Thus (45) may be written

$$\Delta A/2\pi F = \mu\tfrac{1}{2}(T_c-1)^2 + (1-\mu)\,\tfrac{1}{2}(T_h-1)^2. \tag{54}$$

The availability of a cooling machine is, when the temperature drop is not too large,

$$a_c' \equiv a_c/(c_p t_0) = \tfrac{1}{2}(t_c/t_0 - 1)^2, \tag{55}$$

where t_0 and t_c are the temperatures of the gas before entering and after leaving the machine, respectively. As the vortex tube may be said to act as a heating as well as a cooling machine, it is justified to call the value increase $\Delta A/2\pi F$ in (54) the availability of the tube. Thus it must be permissible, at any rate to a first approximation, to compare the efficiency of the tube with other cooling devices through the use of expressions such as (51).

From (51) which is difficult to use in practice, the absolute maximum for the value-increase of a tube, $\Delta A_{\max}$ is easily derived. The condition to be fulfilled is that $-\partial T/\partial\eta(\partial T/\partial\eta - \partial T_{eq}/\partial\eta)$ is a maximum everywhere in the tube; thus

$$\frac{\partial T}{\partial \eta} = \frac{1}{2}\frac{\partial T_{eq}}{\partial \eta} = \tfrac{1}{2}Ec\left(\omega^2 + \frac{1-Pr}{2}\eta\frac{\partial \omega^2}{\partial \eta}\right), \tag{56}$$

which leads to

$$\frac{\Delta A_{\max}}{2\pi F} = \frac{Ec^2}{2Re_h\sqrt{\alpha}}\int_0^1\int_0^1\left(\omega^2 + \frac{1-Pr}{2}\eta\frac{\partial \omega^2}{\partial \eta}\right)^2 \eta\, d\eta\, d\xi. \tag{57}$$

In the simple case where ω, the angular velocity, may be considered as independent of η and ξ

$$\Delta A_{\max}/2\pi F = Ec^2/4Re_h\sqrt{\alpha} \quad \text{or} \quad \Delta A_{\max} = \tfrac{1}{2}\pi l\rho\epsilon_h(v_\infty^2/c_p T_\infty)^2. \tag{58}$$

In two experimental cases (Bruun 1967, 1969; and Scheller & Brown 1957) $\Delta A_{\max}$ is found to be a factor of two and five, respectively, as large as the actual performance of the tubes calculated on the basis of equation (54). (The low efficiency of the second tube is caused by the presence of an unfavourable $\partial T/\partial\eta$ at high ξ, the origin of which is discussed in § 3.)

Thus, equation (57) or (58) permits a relatively simple evaluation to be made of the vortex tube as a temperature separator. The expressions should, however, be used with caution as the various factors are interdependent. For example, an increased turbulent diffusivity would almost certainly lead to smaller tangential velocities, so that the apparent prediction of (58) that improved performance results if the turbulence level is increased, may not be borne out in practice.

4.2. *The turbulent diffusivity*

If (48), referred to region I, figure 1, is written

$$\Delta A/2\pi F = [A(1) - A(0)]/2\pi F \tag{59}$$

with

$$A(\xi)/2\pi F \equiv \left[-\int_0^1 \frac{\partial \psi}{\partial \eta}\tfrac{1}{2}(T-1)^2\, d\eta\right]_\xi, \tag{60}$$

equations (59) and (51) are seen to be alternative expressions for the availability of region I, where only (51) contains the parameter Re_h. Thus, in cases where sufficient temperature and velocity data are available, (51) and (59) combined may provide estimates of Re_h and thereby the turbulent thermal diffusivity. Equation (59) rather than (54) should be used because value-changes outside region I may take place. Estimates of this kind have been made in 5 cases, the results of which are shown in figure 15. Also shown are the equivalent results obtained on the basis of a quantitative analysis of the different terms in (18)

of § 3 over a tube cross-section. A discussion of the accuracy obtained by these two procedures is presented in Linderstrøm-Lang (1970*c*).

The abscissa in figure 15 is the Reynolds number, *Re*, as obtained in § 2 from the axial decay of tangential velocity. Thus the correlation displayed in the figure shows the treatments in §§ 2 and 3 to be mutually consistent as regards turbulent diffusivities.

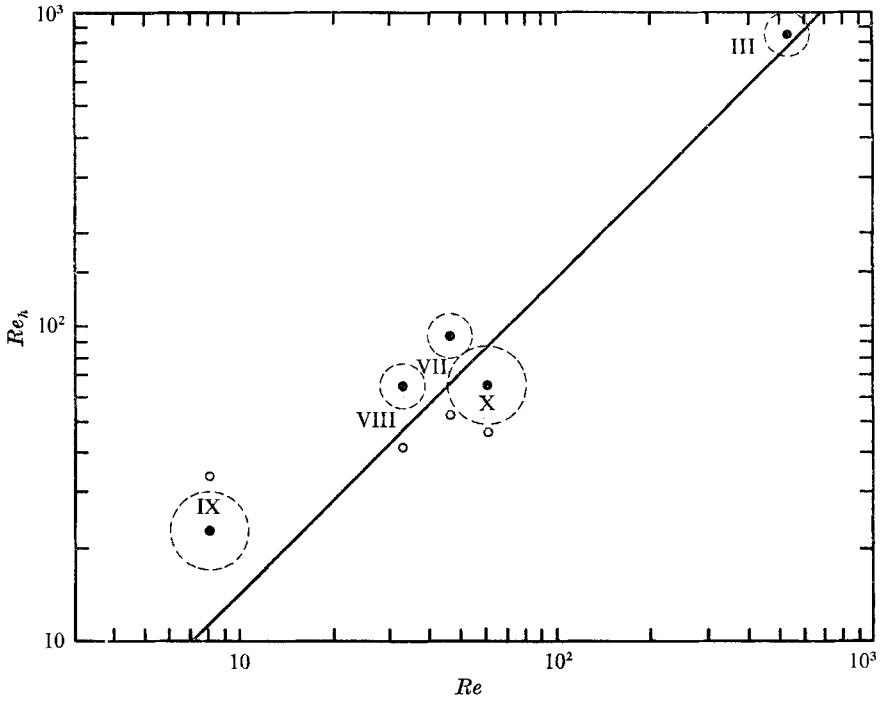

FIGURE 15. Correlation of Reynolds numbers, *Re*, from axial gradient of tangential velocity (§ 2) with Reynolds numbers, Re_h, from temperature distribution (§§ 3 and 4). Roman numerals refer to data in table 1. Solid points, Re_h determinations from value-increase; open points, Re_h determinations from energy equation. Circles around points indicate range of values obtained. The line drawn assumes a turbulent Prandtl number of 0·7.

REFERENCES

ANDERSON, O. L. 1963 Theoretical effect of Mach number and temperature gradient on primary and secondary flows in a jet-driven vortex. *UAC-Research Lab. Report* no. RTD-TDR-63-1098.

BENJAMIN, T. BROOKE 1962 Theory of the vortex breakdown phenomenon. *J. Fluid Mech.* **14**, 593.

BRUUN, H. H. 1967 Theoretical and experimental investigation of vortex tubes. *Dept. of Fluid Mech. Report* no. 67–1, *Danish Techn. Univ.*

BRUUN, H. H. 1969 Experimental investigation of the energy separation in vortex tubes. *J. Mech. Engng Sci.* **11**, 567.

COHEN, K. 1951 *The Theory of Isotope Separation.* McGraw-Hill.

DEISSLER, R. G. & PERLMUTTER, M. 1960 Analysis of the flow and energy separation in a turbulent vortex. *Int. J. Heat Mass Transfer*, **1**, 173.

FULTON, C. D. 1950 Ranque's tube. *Refrig. Engng.* **58**, 473.

GULYAEV, A. I. 1966 Vortex tubes and the vortex effect (Ranque effect). *Soviet Phys. tech. Phys.* **10**, 1441. (Russ. orig. *Zh. Tekh. Fiz.* **35** (1965), 1869.)

HARTNETT, J. P. & ECKERT, E. R. G. 1957 Experimental study of the velocity and temperature distribution in a high velocity vortex-type flow. *Trans. ASME.* **79**, 751.

HILSCH, R. 1946 Die Expansion von Gasen im Zentrifugalfeld als Kälteprozess. *Z. für Naturf.* **1**, 208.

KASSNER, R. & KNOERNSCHILD, E. 1948 Friction laws and energy transfer in circular flow. *Report* PB-110936, parts I and II.

KEYES, J. J. 1961 Experimental study of flow and separation in vortex tubes with application to gaseous fission heating. *J. Am. Rocket Soc.* **31**, 1204.

LAY, J. E. 1959 An experimental and analytical study of vortex-flow temperature separation by superposition of spiral and axial flows, part 1. *Trans. ASME.* **81**, 202.

LEWELLEN, W. S. 1962 A solution for three-dimensional vortex flows with strong circulation. *J. Fluid Mech.* **14**, 420.

LEWELLEN, W. S. 1964 Three-dimensional viscous vortices in incompressible flow. Ph. D. thesis, Univ. of California (University Microfilms, Inc., Ann Arbor, order no. 64-8331).

LEWELLEN, W. S. 1965 Linearized vortex flows. *A.I.A.A. J.* **3**, 91.

LINDERSTRØM-LANG, C. U. 1970*a* Vortex tubes with weak radial flow. Part I. Calculation of the tangential velocity and its axial gradient. *Risö Report* no. 216.

LINDERSTRØM-LANG, C. U. 1970*b* Vortex tubes with weak radial flow. Part II. Calculation of the three-dimensional temperature distribution. *Risö Report* no. 217.

LINDERSTRØM-LANG, C. U. 1970*c* Vortex tubes with weak radial flow. Part III. Calculation of the performance and estimation of the turbulent diffusivity. *Risö Report*, no. 218.

RAGSDALE, R. G. 1961 Applicability of mixing length theory to a turbulent vortex system. *NASA TN* D-1051.

REYNOLDS, A. J. 1961 Energy flows in a vortex tube. *J. Appl. Math. Phys.* **12**, 343.

ROSENZWEIG, M. L., LEWELLEN, W. S. & ROSS, D. H. 1964 Confined vortex flows with boundary-layer interaction. *Report* no. ATN-64(9227)-2. AD 431844.

ROSENZWEIG, M. L., ROSS, D. H. & LEWELLEN, W. S. 1962 On secondary flows in jet-driven vortex tubes. *J. Aero. Sci.* **29**, 1142.

SCHELLER, W. A. & BROWN, G. M. 1957 The Ranque–Hilsch vortex tube. *Ind. Engng Chem.* **49**, 1013.

SCHEPER, G. W. 1951 The vortex tube; internal flow data and a heat transfer theory. *Refrig. Engng.* **59**, 985.

SHAPIRO, A. H. 1954 *Compressible Fluid Flow*, II. New York: The Ronald Press Co.

SIBULKIN, M. 1962 Unsteady, viscous, circular flow. Part 3. Application to the Ranque–Hilsch vortex tube. *J. Fluid Mech.* **12**, 269.

STONE, W. S. & LOVE, T. A. 1950 An experimental study of the Hilsch tube and its possible application to isotope separation. *Oak Ridge Nat. Lab. Report* ORNL 282.

SUZUKI, M. 1960 Theoretical and experimental studies on the vortex tube. *Sci. Pap. Inst. Phys. Chem. Research, Tokyo*, **54**, 43.

TAKAHAMA, H. 1965 Studies on vortex tubes. *Bull. JSME.* **8**, 433.

TAKAHAMA, H. & KAWASHIMA, K.-I. 1960 An experimental study of vortex tubes. *Mem. Faculty Engng Nagoya. Univ.* **12**, 227.